

A Typical Residential Masonry Building in Urban Settlement and its Seismic Assessment

Dipesh Tiwari ^a, Gokarna B. Motra ^b, Kshitij C. Shrestha ^c

^{a, b, c} Department of Civil Engineering, Pulchowk Campus, IOE, Tribhuvan University, Nepal

Corresponding Email: ^a 075msste003.dipesh@pcampus.edu.np, ^b gmotra@ioe.edu.np, ^c kshitij.shrestha@pcampus.edu.np

Abstract

Maximum of masonry buildings in urban areas are with large openings in ground floor level and with different stages of construction adding more non-engineered complexity to the structure. In this paper, the analytical methodology for seismic vulnerability assessment is presented through a case study of existing masonry building in Panauti Municipality with different structural deficiencies. Stepwise procedures of seismic assessment is analyzed through non-linear pushover analysis and fragility functions are generated to define the level of vulnerability of the building. The area elements at potential yielding sections are replaced with Multi-linear plastic non-linear link elements which are defined in finite element software SAP2000. The proposed study has direct implication towards assessing the vulnerability of similar case study of URM residential buildings which further assists for the development of proper retrofitting strategies assuring life safety requirements.

Keywords

Unreinforced Masonry (URM), Nonlinear Link, Pushover, Fragility, Seismic Vulnerability

1. Introduction

Masonry are the widely used structural construction practices made up from individual masonry units laid together with or without the binding material. They represent the non-homogeneous and an-isotropic structural components with varying mechanical properties. Geological formations, availability of resources, quality of materials and workmanship, masonry materials and binding materials used, positioning of openings, age and loading eccentricities and many other various factors affect the property of masonry structure.

We can see many of the historical archaeological structures made up of masonry which are still in existence. Because of locally available construction materials, fire resistant and sound absorption, low maintenance, high durability and relatively cheaper in construction, masonry structures are also typical construction practice in Nepal. Generally, masonry units like stones, clay bricks and concrete blocks are used with mud, cement or lime mortar as binding material. According to survey from UNDP and CBS 2017 [1], most of the Nepalese houses have exterior

walls with bricks/stone bonded in mud mortar (37.6%) whose number is greater in rural areas; about 49.3% in rural and 20.4% in urban areas. And, the number of exterior walls of cement bonded brick/stone houses are in increasing number, which have increased from 33.4% in 2014/15 to 36.6% in 2015/16.

Unreinforced masonry (URM) walls are generally load bearing structures and their stability is governed by their seismic weight. They undergo considerable stages of structural degradation with age, loadings and seismicity. Heavy seismic weight, brittleness of masonry units, poor construction technology, large and random positioning of openings, weak mortar joints, lack of adequate connections, flexible floor diaphragm, rapid and unmanaged development without proper engineering design and quality control have led to greater extent of damage in the recently occurred earthquake. According to the NRA [2] out of 1,047,261 damaged houses surveyed, 78.4% were of low strength masonry, 7.87% cement-mortared masonry and only 3.57% were reinforced concrete houses. Low strength masonry houses were greatly affected in comparison to other typologies in the recent Gorkha Earthquake in 2015. As Nepal lies in

active seismological region, it is thus more clear that many researches and development on this field is of utmost importance.

Miha Tomazevic (1999) [3] has explained in detail about the failure modes of URM walls and Asteris et.al. (2015) [4] has summarized the different analytical approaches of masonry modelling performed by various researchers. There are few researches on masonry structures in the context of Nepal. Maximum of these researches are focused on historical temples presented by Shrestha et.al. (2017) [5] ; and in masonry school buildings by Giordano et.al. (2019) [6]. Similarly, Gautam et. al. (2018) [7] in their paper proposed a new damage data for deriving the fragility functions for RC, brick masonry, and stone masonry buildings. Their results suggest that most of the masonry buildings in Nepal are susceptible of high vulnerability in seismic excitation.

Further, addition of extra storey in the existing masonry building with increase in family size and financial support is pretty common in developing parts of rural-urban/ semi-urban parts on Nepal. Even the construction technique and materials vary within these storey levels adding more complexity to the structure. Similarly, large openings in the ground floor, and in front face, are made for business purpose, making the lower storey stiffness weaker than upper stories. Cracks originate from these openings corners concentrating larger local strain energy, resulting the collapse of whole structure. Thus, it is of prime importance to check the seismic performance of these buildings in their existing conditions and carry out necessary strengthening measures to control the risk of life and property. This paper focus on a case study of existing URM building. Stepwise procedures of seismic assessment is analyzed through non-linear pushover analysis and fragility functions are generated. The proposed study has direct implication towards assessing the vulnerability of similar case study URM residential buildings.

2. Non-linear link elements and model validation for its use

2.1 Non-Linear (NL) Link Element

A link is defined as the two joint connecting element. According to the properties assigned to the element and the analysis being performed, link can exhibit different types of behavior, namely: linear, nonlinear, or frequency-dependent [8]. The Non-Linear (NL)

link element allows modelling the material non-linearity through user defined force versus deformation relationships, which are defined in this study as Multi-linear plastic non-linear links. The potential yielding regions of the interface of wall segments of the building are replaced with non-linear links and the area elements outside these assumed yielding regions are provided with linear-elastic area elements which are modelled using their full gross-sectional properties. For addressing the secondary moment generated, a rigid line element is added in a way that the links associated generate a secondary moment at only one end of these links [9].



Figure 1: Nonlinear Link Definition for URM Wall, Axial Direction

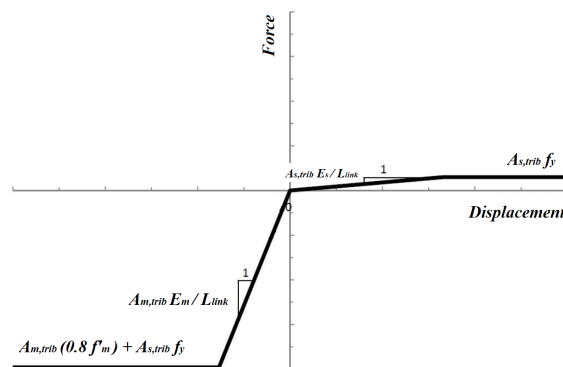


Figure 2: Nonlinear Link Definition for Reinforced Masonry Wall, Axial Direction

The force versus deformation data is obtained from the tributary area of wall elements being represented by the nonlinear links. In compression, the initial stiffness value is obtained from tributary area, modulus of elasticity of masonry and the length of the non-linear link (fig:1). Analogously, the steel reinforcement rigidity and the length of non-linear link determines the initial stiffness in tension, in case of reinforced masonry (fig:2).

Similarly, the force versus deformation relationship are defined as bi-linear and symmetrical for simulating the response in shear. The first linear line (fig:3) is defined by the stiffness based on gross section properties and the horizontal second line represents constant force i.e. the nominal shear strength of the wall segment which is taken under considerations.

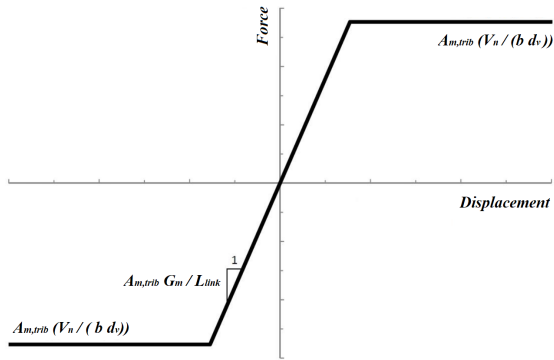


Figure 3: Nonlinear Link Definition, Shear Direction

2.2 Model Validation

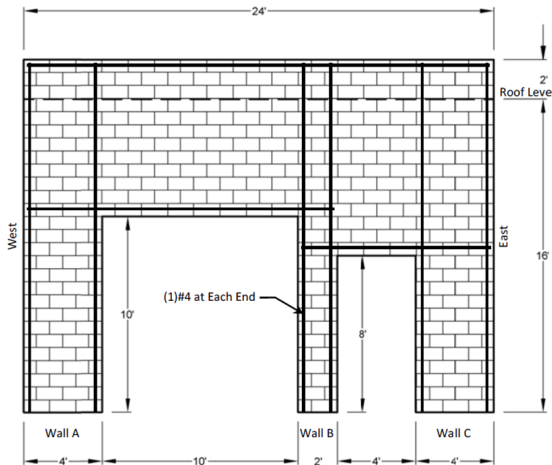


Figure 4: Description of Wall Considered, Lepage and Sanchez [9]

The proposed 2D simplified model as suggested by Lepage and Sanchez (2012) [9] were applied to a planar one-story reinforced masonry wall with two openings (fig:4) and FEM model was prepared in SAP 2000 v23 (fig:5(b)). Non-linear links were provided in potential yielding sections, which can be taken as the corners of the openings with higher stress concentrations and the path that the cracks can propagate through. And, outside areas were modelled as linear elastic area elements using their gross section properties and the relevant output results from non-linear static pushover analyses were compared.

The yield strength of reinforcement bar taken is 410 MPa (60 ksi) and masonry compression strength is 10 MPa (1500 psi). The output data from pushover analyses as proposed by Lepage and Sanchez [9] were compared to the output from a refined computer model developed in SAP2000 (fig:6). Results of the comparison, as shown in fig:6 indicate that the proposed models were sufficiently accurate. This comparison helps us to better understand the use of Non-Linear Multi-Plastic Link Elements.

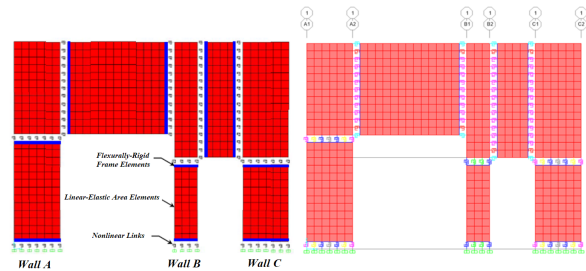


Figure 5: (a) Non-Linear Link Positioning as Suggested by Lepage and Sanchez [9], (b) Model Prepared in SAP2000

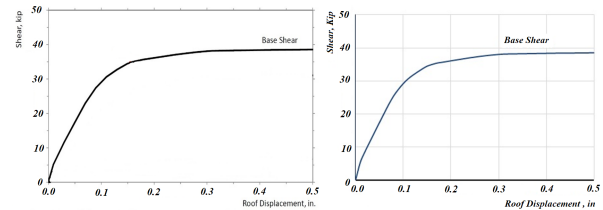


Figure 6: (a) Base Shear versus roof displacement for Non-linear Link Model, Eastward Loading, Lepage and Sanchez [9], (b) Pushover Curve (Shear vs Roof displacement) obtained from SAP 2000

This suggests the non-linear links can be used for replacing the area elements. Their location would be based on the visual assessment of the building under study and in accordance with the observed crack patterns in the actual structure.

3. Methodology

3.1 General Building Description

A case study of three and a half storied unreinforced masonry building in Panauti Municipality, ward no - 4, Kavrepalanchowk district (32 Km South-East of Kathmandu) is selected for the case study. The building prototype selected represents the typical building found in the urban settlement of Panauti

Municipality. The important parameters required for analyzing the vulnerability of the building are measured and recorded from the visual assessment and survey questionnaire (details in Table:1). Photographs are also used as cross reference for preparing as-built architectural drawings and to access damages incurred in the latest earthquake.

Table 1: General Building Description

Building Typology	Ordinary Load Bearing Masonry Residential Building
Age	First and second storey : 35 years Third and fourth storey : 20 years
No. of Stories	Three and half
Storey Height	8' (2.45m)
Total Height	32' (9.75m)
Plan	L = 16' 3" (4.95m) B = 17' (5.18m)
Wall :	
First and second Floor	Back Face: BMM (14" (0.36m)) All other grids: BCM (12" (0.3m))
Third and Fourth Floor	Back Face: BCM (12" (0.3m)) All other grids: BCM (12" (0.3m))
Floor:	
First and second Floor	Flexible floor diaphragm with Timber frames and mud finishing
Third and Fourth Floor	Rigid floor diaphragm with RCC Slab
RCC Beams:	
First and second Storey	9" * 9" RCC (0.23m x 0.3m) (Along A-A only)
Third and Fourth Storey	9" * 12" RCC (0.23m x 0.3m) (Along A-A Only)

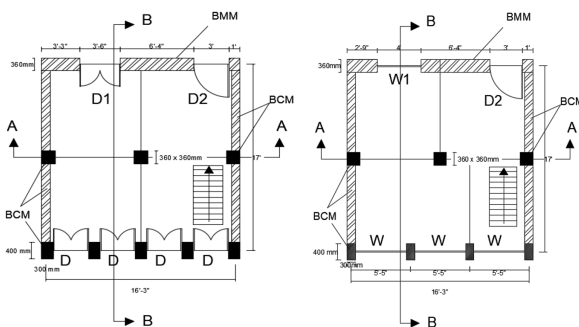


Figure 7: (a) Ground Floor Plan (b) First Floor Plan

These collected data were then referred to prepare the building plans (fig:7), elevations, sections (fig:8); and a complete drawing was developed which provided the basis for finite element modelling.



Figure 8: (a) Section at A-A, (b) Front View, (c) Section at B-B

The front face of the building consists of five masonry piers of size 0.3m x 0.4m in ground storey with doors of size 3' x 7' in between them. These corner piers are extended up to the roof level but load path of middle piers is discontinuous at first storey level. Three windows of size 5' x 5' are placed in between piers at front face of second and third storey levels. Beams are projected radially (Along A-A) from the central masonry pier of size 0.36m x 0.36m whose other ends are supported over similar piers placed at corners. These piers are made up of Brick Masonry in Cement Mortar (BCM). The left and right side of the building are 0.3m thick BCM walls with no openings. But, the back face of the building is made of Brick Masonry with Mud Mortar (BMM) up to the second storey level and is 0.36m thick.

3.2 Finite Element Modelling

The case study building is modelled in Finite Element Software [8], SAP 2000 v23.1.0 (fig: 9). A 3D discontinuum macro-modelling approach is adopted to model the building at present condition. The wall components are modelled as thick shell elements and the slab floors as thin shell area elements. The first floor consists of wooden floor with mud covering. The storey floor levels made up of RCC slab is assigned to be rigid diaphragm and timber floor level in first storey to be flexible, which is modelled as equivalent slab of 125mm with self weight equal to the dead loads of joists and planks. The structural wall members of the model has both BMM and BCM elements. Meshing is done at 6" x 6" to increase accuracy. The foundation is assumed to be rigidly fixed at ground level. The model consists of 11879 nodes, 11567 areas and 46268 edges. The self weight of BMM is taken as 17.68 kN/m³ and BCM as 20 kN/m³. The dead weight of RC slab is taken 25 kN/m³ and timber as 8 kN/m³. Floor finish is taken 1 kN/m². Live loads on floor is 2 kN/m² and

1.5 kN/m² on roof. Because of lack of actual field data and material testing, all mechanical properties of materials in the building is taken from relevant past literatures that accounts for the present study.

Table 2: Concrete Properties

Concrete grade for Beams / Floor / Roof slab	M20 (20MPa)
Modulus of Elasticity ($5000\sqrt{f_{ck}}$)	22 GPa
Poisson's Ratio	0.2

Table 3: Brick Masonry in Cement Mortar (BCM)

Compression Strength of Masonry	4.1 MPa
Modulus of Elasticity	2,300 MPa
Poisson's ratio	0.25
Modulus of Rigidity	920 MPa
Shear Strength	0.25 MPa

(Source: Kaushik et. al. [10])

Table 4: Brick Masonry in Mud Mortar (BMM)

Compressive Strength of Masonry	1.82 MPa
Young's Modulus	509 MPa
Poisson's ratio	0.25
Modulus of Rigidity	204 MPa
Shear Strength	0.15 MPa

(Source: Parajuli [11])

Table 5: Flexible Floor Diaphragm (Timber Slab)

Wood Type	Sal Wood
Modulus of Elasticity	12,500 MPa
Poisson's ratio	0.12
Density	0.8 kg/m ³
Shear Rigidity	1,500 MPa

(Source: Shrestha et. al. [5])

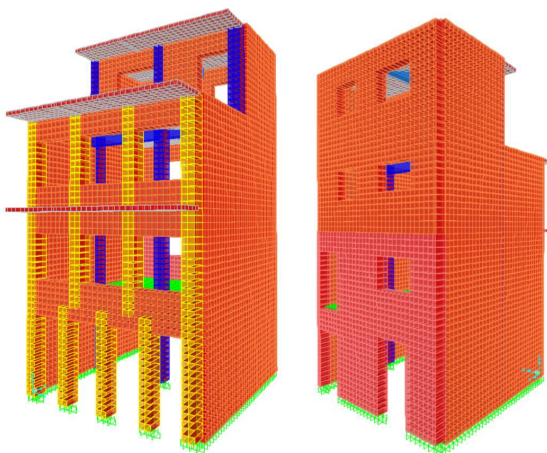


Figure 9: 3D FEM Model (a) Front and Right Side View (b) Back and Left Side View

The link parameters were calculated based on the gross section properties of area elements which are replaced by Multi-linear plastic nonlinear links at potential yielding sections. The force-deformation curve is taken to be bi-linear plot (sample example is shown in table 7 and 8). The tensile stress of masonry is taken 5% of its compressive stress. A total of 8 different link types were defined based on material sectional properties, tributary areas and their positioning on centres and ends (Table: 6). End links are provided at nodal ends of the cracks origination and centre links at central nodes of meshed wall.

Table 6: Initial stiffness values for NL-Link (kN/m)

Link Properties (Material-Thickness)	Axial (U1)	Shear (U2, U3)
BCM – 0.3m- Centres	690000	276000
BCM – 0.3m- Ends	345000	138000
BCM – 0.36m- Centres	828000	331200
BCM – 0.36m- Ends	414000	165600
BCM – 0.4m- Centres	920000	368000
BCM – 0.4m- Ends	460000	184000
BMM – 0.36m- Centres	183240	73440
BMM – 0.36m- Ends	91620	36720

Table 7: Axial(U1) Force-displacement plot: Bilinear (BCM - 0.3m - Centres)

Displacement(m)	Force(kN)
-0.00272	-187.45
-0.00027	-187.45
0	0
0.0000136	9.37
0.00014	9.37

Table 8: Shear(U2) and (U3) Force-displacement plot: Bilinear (BCM - 0.3m - Centres)

Displacement(m)	Force(kN)
-0.00041	-11.43
-0.00004	-11.43
0	0
0.00004	11.43
0.00041	11.43

3.3 Positioning of NL-Links

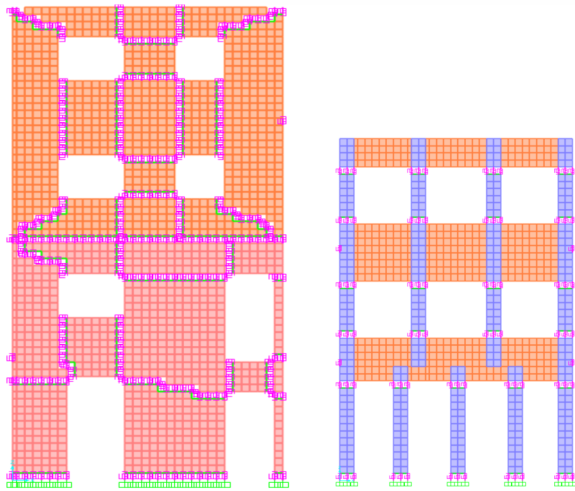


Figure 10: Link Positioning at: (a) Back Side View: In-Plane (b) Front View: In-Plane

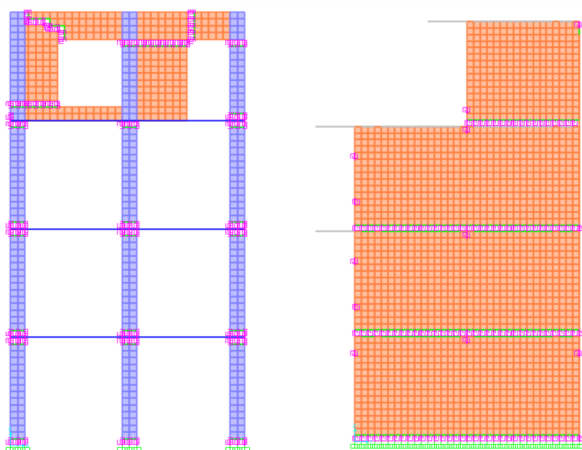


Figure 11: Link Positioning at: (a) Mid-Sectional View : In-Plane (b) Side Views (Left and Right) : Out of Plane

The positioning of NL-Links is based on the visual assessment of the building under study, and in accordance with the observed crack patterns in the actual structure. Different trails were performed and the best critical positioning that perfectly describes the building non-linearity was chosen as illustrated in fig: 10 and 11. A total of 700 NL-Links are provided, and as minimum as possible assuming in-plane along X-direction. This reduces the computational time and complexity in modelling.

4. Results and Discussion

4.1 Equivalent Static Analysis

The fundamental time period before the introduction of link elements was 0.303 sec and after the introduction of link is 0.321 sec, which are within the closer range. The modal participating mass ratio in 1st mode is 85.4% along X-direction.

4.2 Pushover Analysis

Pushover analysis estimates maximum global displacement of the existing buildings, and its seismic capacity to prepare different retrofit design guidelines. For brevity and simplicity, pushover in only one direction (along X – Axis) is presented in the study. Further, the direction also represents the weaker side of the building with presence of majority of openings along the in-plane loaded walls. Initially, nonlinear gravity load case is defined to start with zero initial conditions, and then push load case is defined to continue from the NL gravity case. The control node is taken at centre of mass at roof level. The obtained pushover curve is shown in fig:12.

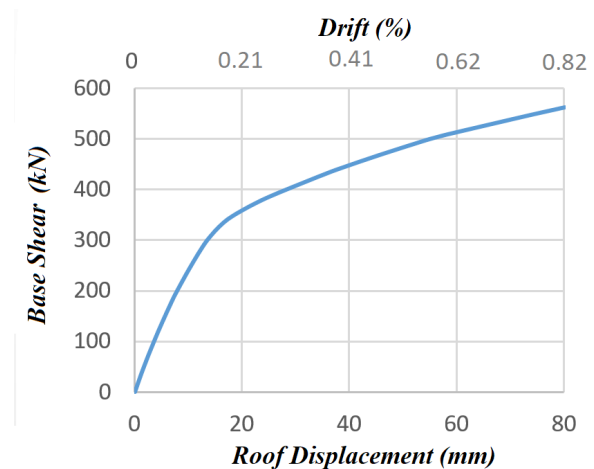


Figure 12: Pushover Curve

4.3 Capacity Spectrum Method (CSM)

The Pushover curve thus obtained is converted to the capacity spectrum of Spectral Acceleration S_A versus Spectral Displacement S_D relationship represented by an Equivalent Single Degree of Freedom (ESDOF) System [12].

$$S_A(T) = \frac{V_B}{M} \quad (1)$$

Where, V_B represents the seismic base shear, and M is the effective modal mass given by:

$$M = \frac{L_n^2}{M_n} = \frac{(\sum m_i (\delta_{i1}))^2}{\sum m_i (\delta_{i1})^2} \quad (2)$$

Also,

$$S_D(T) = \frac{D_R}{\beta} = \frac{(\delta_{i1})^T [m] (\delta_{i1})}{((\delta_{i1})^T [m] (1))} \quad (3)$$

Where, displacement vector of first mode is given by: $(\delta)_1 = (\phi)_1 \beta_1 S_D(T)$ And, $[m]$ is the lumped floor mass matrix.

Similarly, the input response spectrum curves in SA - T, resulting from input parameters of certain earthquake intensity, is converted to Acceleration-Displacement Response Spectrum (ADRS) plot by the relation:

$$S_D(T) = \left(\frac{T}{2\pi} \right)^2 S_a(T) \quad (4)$$

With the demand spectrum and the capacity curve in same domain of spectral acceleration and spectral displacement (ADRS format), we calculate the performance point according to steps proposed by Otani et.al. (2000) [12]. Two response spectra from IS 1893:2016 and NBC 105:2020 were chosen for this study. All the steps followed for converting the capacity curve and demand curve for obtaining the performance point and to generate fragility curves, was performed through MATLAB programming.

A sample example for the determination of performance point with PGA 0.2g of IS 1893:2016 and PGA of 0.2g of NBC 105:2020 for hard soil response spectrums is shown in fig: 13.

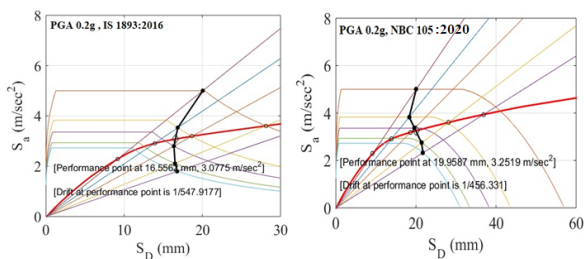


Figure 13: Determination of performance point using CSM (a) For PGA of 0.2g of IS 1893-2016, (b) For PGA of 0.2g of NBC 105:2020

A single performance point is obtained for one PGA level of the particular earthquake spectrum. A similar procedure is followed to obtain performance points for different PGA levels of different sources of earthquake response spectra.

4.4 Fragility Curves

The CSM analysis for various ground motion parameters gives us a set of different values of performance point. These results can be correlated to a damage state, expressing the vulnerability of a structure to a user-defined intensity measure, as a graphical function of capacity curve. This fragility curve expresses the probability of exceedance of a specified damage stage as a function of input earthquake intensity parameters like: PGA, PGV, SA, etc. For the generation of fragility curves in the present study, methodology proposed by Wen et al. (2004) [13] have been used. Probability that the structure exceeds limit damage state for a given Ground Motion Intensity (GMI) is given by the formula:

$$P(LS_i/GMI) = 1 - \phi\left(\frac{\lambda_{cl}^i - \lambda_{D/GMI}}{\beta_{D/GMI}}\right) \quad (5)$$

Where the mean $\lambda_{D/GMI}$ and standard deviation $\beta_{D/GMI}$ parameters are defined by:

$$\lambda_{D/GMI} = \ln(a_1) + a_2 \ln(GMI) \quad (6)$$

$$\beta_{D/GMI} = \sqrt{\frac{\sum_{k=1}^n [\ln(GMI_k) - \lambda_{GMI}(GMI_k)]^2}{n - 2}} \quad (7)$$

The constants a_1 and a_2 are obtained through linear regression analysis as the logarithmic plot of storey drift and ground motion intensity parameters in terms of PGA (fig: 14.)

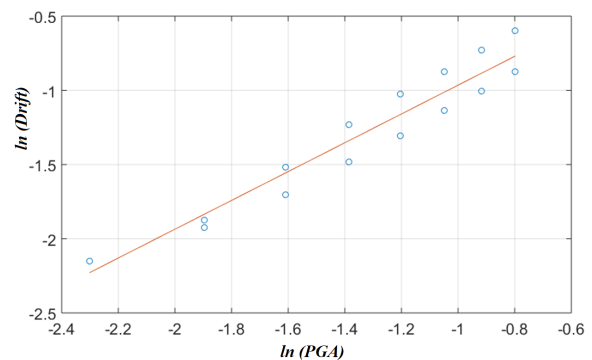


Figure 14: Regression plot

Three categories of limit states: Immediate Occupancy Level (IO), Life Safety Level (LS) and Collapse Prevention Level (CP) are specified for

generating the fragility curves. The different threshold values are assigned for the target structure from the structural viewpoint, which is similar to FEMA 273 [14].

Immediate Occupancy (IO) = 1/750 (i.e. 0.13% drift)

Life Safety (LS) = 1/500 (i.e. 0.2% drift)

Collapse Prevention (CP) = 1/250 (i.e.0.4% drift)

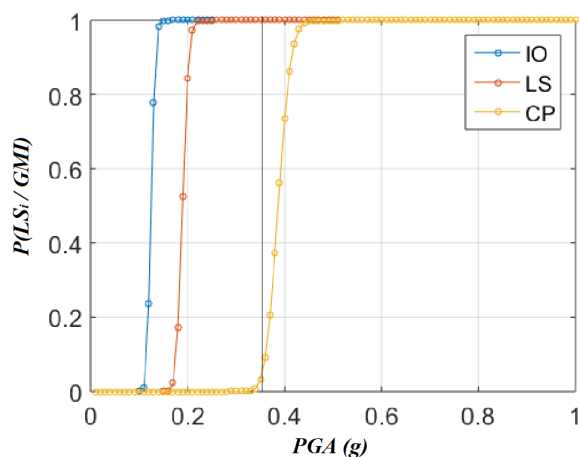


Figure 15: Fragility Curve

From graph (fig: 15), we can observe, at 0.2g PGA, building has 80% exceedance probability of life safety level (LS) and for 0.4g PGA, building has 80% exceedance probability of collapse prevention level (CP). For 0.35g PGA, that corresponds to the seismic zoning factor of 0.35g with 475 years return period for Panauti Municipality as defined by NBC 105: 2020, the probability of exceedance of the IO, LS and the CP limit states is 100%, 100% and about 5%. It is thus evident that the building taken into consideration is in risk for life safety.

5. Conclusions

From the analysis of fragility curves, we can clearly see that the URM building under consideration is vulnerable of future probable earthquakes. The present study helps to better understand the seismic vulnerability assessment of masonry buildings. And, to ensure safety of life and property further retrofitting strategies are to be recommended. Authors' future works will focus on extending the current model to propose the seismic retrofitting measures for selected prototype URM building.

Acknowledgments

The present work is partially supported by the project “Nepal Homes and Communities, Baliyo Ghar Baliyo

Sahar” with primary focus on unreinforced masonry walls with mixed typology in Panauti Municipality.

References

- [1] UNDP and CBS Nepal. Annual household survey 2015/2016. 2016.
- [2] National Reconstruction Authority (NRA). A journal of development. 2021.
- [3] Miha Tomazevic. *Earthquake-Resistant Design of Masonry Buildings*. Imperial College Press, 1999.
- [4] Panagiotis Asteris, Vasilis Sarhosis, Amin Mohebkhah, Vagelis Plevris, Loizos Papaloizou, Petros Komodromos, and Jose Lemos. *Numerical Modeling of Historic Masonry Structures*, pages 213–256. 2015.
- [5] Sujan Shrestha, Bipin Shrestha, Manjip Shakya, and Prem Nath Maskey. Damage assessment of cultural heritage structures after the 2015 gorkha, nepal, earthquake: A case study of jagannath temple. *Earthquake Spectra*, 33(1-suppl):363–376, 2017.
- [6] Nicola Giordano, Flavia De Luca, Anastasios Sextos, and Prem Nath Maskey. Derivation of fragility curves for urm school buildings in nepal. 2019.
- [7] Dipendra Gautam, Giovanni Fabbrocino, and Filippo Santucci de Magistris. Derive empirical fragility functions for nepali residential buildings. *Engineering Structures*, 171:617–628, 2018.
- [8] Computers and structures Inc. *Structural Analysis and Design*.
- [9] Andres Lepage and Reynaldo Sanchez. Practical nonlinear analysis for limit design of reinforced masonry walls. *The Open Civil Engineering Journal*, 2012:107–118, 11 2012.
- [10] Hemant B. Kaushik, Durgesh C. Rai, and Sudhir K. Jain. Stress-strain characteristics of clay brick masonry under uniaxial compression. *Journal of Materials in Civil Engineering*, 19(9):728–739, 2007.
- [11] H. Parajuli. Determination of mechanical properties of the kathmandu world heritage brick masonry buildings. 2012.
- [12] S. Otani, H. Hiraishi, M. Midorikawa, and M. Teshigawara. New seismic design provisions in japan. 197:87–104, 2002.
- [13] Y. Wen, Bruce Ellingwood, and Joseph Bracci. Vulnerability function framework for consequence-based engineering. 2004.
- [14] FEMA - 273. *NEHRP Guidelines for the Seismic Rehabilitation of Buildings*.